Layer-by-layer nucleation mechanism for quantum dot formation in strained heteroepitaxy

Ruoxi Xiang, M. T. Lung, and Chi-Hang Lam

Department of Applied Physics, Hong Kong Polytechnic University, Hung Hom, Hong Kong, China
(Received 4 June 2009; revised manuscript received 20 October 2009; published 2 August 2010)

We study the spontaneous formation of quantum dots in the form of three-dimensional (3D) islands on faceted surfaces in heteroepitaxy. Island development from fast kinetic Monte Carlo (KMC) simulations at low deposition rates is found to follow a layer-by-layer nucleation pathway characterized by energetics driven continuous lateral expansion interrupted by a sequence of independent two-dimensional (2D) upper-layer nucleation events. The process involves only unstable 2D upper-layer nuclei but no unstable 3D nucleus. We have calculated analytically the elastic strain energy of an island in the form of an axisymmetric stepped mound using a small-slope approximation. The total free energy of a system with a 3D island and an adatom bath is obtained. Our theory explains island formation via a free energy driven layer-by-layer nucleation mechanism. Upper-layer nucleation energy barrier, nucleation time, critical radius, and island step spacings are estimated. The relevance of entropic step-step repulsion is discussed. Our theory satisfactorily explains the 3D KMC simulations and may describe the initial evolution of islands in the form of stepped mounds observed in experiments.

I. INTRODUCTION

Heteroepitaxial growth refers to a kind of epitaxy in which the materials constituting the substrate and the film are different. The lattice constants of the film and the substrate are in general different and the film is thus intrinsically stressed. Nano-structures which allow more effective relaxation of the strain energy are energetically favorable. An important example is the self-assembly of three-dimensional (3D) islands, which can behave as quantum dots and have potential applications in optoelectronic devices [1–4]. A widely studied system is Ge, or more generally the alloy Ge_xSi_{1-x} deposited on Si(100) substrates with a $4x\%$ lattice misfit [5,6]. During deposition, islands of pyramidal or hut geometries bounded by (105) facets form spontaneously. At relatively low temperature and high misfit, it is suggested that islands form via a 3D nucleation process in which subcritical 3D islands grow and become stable after overcoming an energy barrier [7]. At relatively high temperature or low misfit, experiments have clearly demonstrated that pyramid formation is preceded by unfaceted shallower pre-pyramids or shallow stepped mounds [8–13]. Tersoff *et al.* argued that the $Ge_xSi_{1-x}(100)$ surface is not a true facet so that the strain induced surface instability leads to the formation of the prepyramids [10]. Sutter and co-workers alternatively suggested that islands form via the strain induced evolution of stepped mounds on faceted (100) surface without involving any 3D nucleation barrier [11,12].

The distinct dynamics of island formation on unfaceted and faceted surface under deposition conditions have been illustrated using kinetic Monte Carlo (KMC) simulations in 3D for 8% misfit [14]. At 1000 K above the roughening transition temperature of about 750 K for the model, the surface is unfaceted and surface steps are abundant. Islands have rounded tops and consist of layers with very rugged edges during their initial development. A closer examination on the morphological data reveals that the uppermost layers randomly grow and dissolve many times and become stabi-

lized only after being covered by further layers on top. The steady development of the islands implies that there is no macroscopic energy barrier in the island formation process. The dynamics is instead driven by a strain induced instability [1] as suggested in Ref. [10]. At 600 K, the surface is faceted. Islands are truncated cones. Upon deposition, an island first expands laterally and then a new layer nucleates on top. The dynamics follows essentially a layer-by-layer nucleation mechanism analogous to that for the formation of pits during annealing [14]. For both temperatures considered, there exist no single-step 3D nucleation barrier consistent with experimental findings on systems with nominal misfit varying from 1 to 4% [8–13].

In this work, we develop a detailed theoretical description for the formation of 3D islands via the layer-by-layer nucleation mechanism. We show that it satisfactorily explains KMC simulation results at 600 K below the roughening transition temperature at low deposition rates corresponding to the quasi-equilibrium limit. The remainder of this paper is organized as follows. Section II describes the KMC simulation model and the morphological evolution of a typical island. Next, the island strain energy and the total free energy of the system are calculated analytically in Sec. III and Sec. IV respectively. In Sec. V, we compare our theoretical results with KMC simulations. We conclude this paper in Sec. VI with further discussions.

II. KINETIC MONTE CARLO SIMULATIONS

Fast KMC simulations based on lattice ball and spring models for elastic solids [15] have allowed large scale computational studies on the dynamics of island formation in strained heteroepitaxy in both 2D [16–19] and 3D [14,20–22]. KMC methods are unique for studying properties for which fluctuations and atomic discreteness are important. Continuum calculations, though very successful in investigating unstable island growth [23,24], cannot naturally account for fluctuations relevant to nucleation events. The

much more accurate *ab initio* [25–27] and molecular dynamics [28,29] approaches are however too computationally intensive for dynamical studies in sufficiently large scales.

Following Ref. [14], the parameters in our ball and spring model are based on the Ge/Si(001) system extrapolated to a misfit $\varepsilon = 8\%$. Since typical island size and formation time scale is known to decrease with increasing lattice misfit, we have chosen this rather large value so that the whole island formation process can be simulated with reasonable computer run time. It is based on a cubic lattice with a substrate lattice constant $a_s = 2.715$ Å so that a_s^3 gives the correct atomic volume in crystalline silicon. The lattice constant a_f of the film material is related to the lattice misfit $\epsilon = (a_f - a_s)/a_f$. Nearest and next nearest neighboring atoms are directly connected by linear elastic springs with force constants $k_1 = 2eV/a_s^2$ and $k_2 = k_1$, respectively. The elastic couplings of adatoms with the rest of the system are weak and are completely neglected for better computational efficiency. Solid-on-solid conditions and atomic steps limited to at most one atom high are assumed. Every topmost atom in the film can hop to a different random topmost site within a neighborhood of $l \times l$ columns with equal probability where $l = 7$. The maximum hopping distance $3\sqrt{2}$ is smaller than the diameters of the typical islands to be studied and we have checked in simulations at higher deposition rates that taking $l = 3$ gives similar results. The hopping rate Γ_m of a topmost atom m follows an Arrhenius form:

$$\Gamma_m = R_0 \exp\left[-\frac{n_{1m}\gamma_1 + n_{2m}\gamma_2 - \Delta E_m - E_0}{k_B T} \right]. \qquad (1)$$

Here, n_{1m} and n_{2m} are the numbers of nearest and next nearest neighbors of atom m. We take $\gamma_1 = 0.085$ eV and $\gamma_2 = \gamma_1/2$. The energy ΔE_m is the difference in the strain energy E_s of the whole lattice at mechanical equilibrium when the site is occupied versus unoccupied. Weakly bonded or highly stressed atoms are hence more likely to hop. The algorithm follows detailed balance. We put $E_0 = 0.415$ eV and $R_0 = 2D_0/(\sigma a_s)^2$ with $D_0 = 3.83 \times 10^{13}$ A² s⁻¹ and $\sigma^2 = l^2/6$ [14].

We have simulated deposition at temperature $T = 600$ K onto an initially flat substrate with $L \times L$ sites using fast algorithms explained in Refs. [14], [20], and [21]. At this temperature, the (100) surface is facetted. We aim at studying the evolution of a single isolated island on the substrate. This allows convenient numerical computation of the island elastic energy and also simplifies comparison with theory to be discussed later. It is also directly relevant to the initial stage of realistic deposition when island density is low. We consider slow deposition at rate $R \leq 10$ ML s⁻¹ and use a lattice with $L = 32$ so that only a single dominant 3D island will emerge in our system. Furthermore, for the coverage considered, islands are small compared with the substrate so that they are well separated from their periodic images resulting from the use of periodic boundary conditions. Interisland elastic interactions at such low coverage are known to be negligible [30]. For the low-deposition rates considered here, the morphologies observed depend mainly only on the coverage θ implying that the evolution is close to the quasiequilibrium limit.
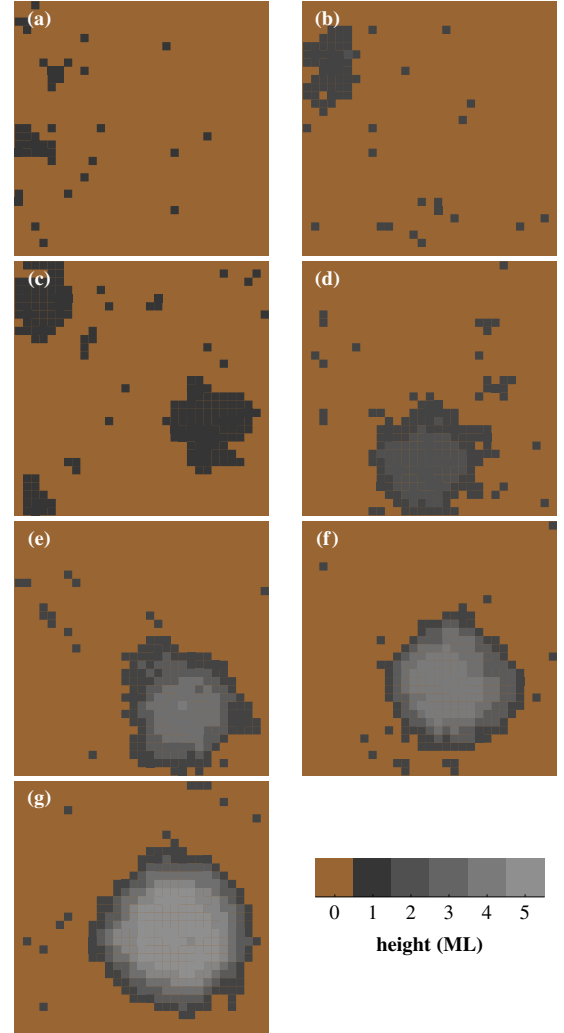

FIG. 1. (Color online) Snapshots from simulation of deposition at rate 1 ML s⁻¹, temperature 600 K, and coverage $\theta = 0.04$(a), 0.07(b), 0.12(c) 0.25(d), 0.36(e), 0.50(f), and 0.94(g).

Figure 1 shows snapshots of a surface from a typical run at $R = 3$ ML s⁻¹. Initially, there are only adatoms and few other subcritical 2D islands as shown in Fig. 1(a). Next, a small 2D stable island emerges [Fig. 1(b)]. We observe additional 2D islands as more atoms are deposited [Fig. 1(c)]. Later, a new layer of atoms nucleates on top of one of the 2D islands leading to a two-layer 3D island. Other 2D islands then dissolve and their atoms all diffuse into the 3D island [Fig. 1(d)]. Upon further deposition, the island continues to grow three dimensionally and the sidewall also becomes steeper [Figs. 1(e)–1(g)].

The development of the 3D island in Fig. 1 follows a layer-by-layer nucleation mechanism. Islands with two layers or beyond are stable as we have never observed their dissolution even if the atomic flux is switched off. In particular, the top layer itself in a two-layered or taller island is stable after attaining a certain size. During deposition, an island gradually expands laterally. Small 2D subcritical upper-layer embryos form and dissolve frequently on top of the island. Only after attaining a certain size with about a few dozen atoms, they become stable and grow steadily leading

to a new upper layer. The development of an upper layer is associated with a slight shrinkage of the lower layers as some atoms are being transferred upward until the island approaches its equilibrium truncated conical shape. This gradual lateral island expansion interrupted by a sequence of sudden 2D upper-layer nucleations characterizes the over growth process of a 3D islands. In all the growth conditions we have studied using our current KMC model, we have not observed any unstable 3D embryo associated with a single-step 3D nucleation process.

III. ELASTIC ENERGY CALCULATION

In this section, we analyze the elastic strain energy of axisymmetric islands in the form of stepped mounds. We treat the system as a continuum elastic solid. The substrate and the deposited material are assumed to have the same elastic constant for simplicity. The compressive stress on the film material can equivalently be represented by effective force monopoles with a line density [2]

$$F(r) = \frac{\varepsilon a_s Y}{1 - \nu} \hat{n}(r) \tag{2}$$

acting at position r on every surface step along the normal direction $\hat{n}(r)$ pointing toward the lower terrace. Here, ν is the Poisson's ratio and Y is the Young's modulus. For our KMC model, their values are $\nu = k_2/(k_1 + 3k_2)$ and $Y = (k_1^2 + 5k_1 k_2 + 4k_2^2)/[a_s(k_1 + 3k_2)]$. We use a small-slope approximation which is valid for gentle surfaces so that the αth component of the displacement $u_\alpha(r)$ at position r induced at the film surface can be written as [31]

$$u_\alpha(r) = \int dr' G_{\alpha\beta}(r - r') F_\beta(r'), \tag{3}$$

where the integral is over all surface steps and $G_{\alpha\beta}$ is the half-space elastic Green's function [32]. The strain relaxation energy E_s which is the total strain energy in the film-substrate system compared with that in the homogeneously strained state can be written as

$$E_s = -\frac{1}{2} \sum_{\alpha,\beta} \int dr dr' G_{\alpha\beta}(r - r') F_\alpha(r) F_\beta(r'). \tag{4}$$

For a 2D circular island of radius R, Eq. (4) gives [3]

$$E_s(R) = -2\pi R\zeta \ln\frac{R}{a_r}. \tag{5}$$

Here, a_r is a spatial cutoff parameter of the order of the single step height which equals the lattice constant a_s. Its value depends on the detailed structure of the surface step. In Eq. (5), ζ is defined by

$$\zeta = \frac{(1 - \nu^2)F^2}{\pi Y}, \tag{6}$$

where $F = |F|$ and its value follows from Eq. (2).

For 3D islands, we approximate them as axisymmetric stepped mounds consisting of n concentric circular layers.

Let R_i be the radius of the ith layer counting from below. The strain energy $E_s(\{R_i\})$ of the island as a function of the set of radii $\{R_1, R_2, \ldots, R_n\}$ can be calculated using Eq. (4) and we obtain, after some straightforward algebra [33]

$$E_s(\{R_i\}) = \sum_{i,j=1}^{n} A(R_i, R_j), \tag{7}$$

where the pairwise interaction term $A(R_i, R_j)$ is defined as

$$A(R_i, R_j) = -\frac{2\pi\zeta}{R_i + R_j} \left\{ -(R_i + R_j)^2 E\left[\frac{4R_i R_j}{(R_i + R_j)^2}\right] \right.$$
$$\left. + (R_i^2 + R_j^2)K\left[\frac{4R_i R_j}{(R_i + R_j)^2}\right] \right\}. \tag{8}$$

We have defined

$$K(x) = \int_0^{\pi/2 - \theta_c} \frac{d\theta}{\sqrt{1 - x\sin^2\theta}} \tag{9}$$

$$E(x) = \int_0^{\pi/2 - \theta_c} \sqrt{1 - x\sin^2\theta}\, d\theta. \tag{10}$$

If a vanishing value is assumed for the angular cutoff θ_c, $K(x)$ and $E(x)$ reduce to the complete elliptic integrals of the first and the second kinds respectively. In our calculation, a finite θ_c of similar magnitude to a_s/R_i and a_s/R_j is needed to suppress a singularity in $K(x)$ at $x = 1$ corresponding to $R_i = R_j$. Specifically, we put

$$\theta_c = \frac{2a_r}{e^2 \max\{R_i, R_j\}}, \tag{11}$$

so that E_s calculated using Eqs. (7)–(11) for a 2D island with $n = 1$ reduces identically back to Eq. (5). Furthermore, this choice preserves the symmetry $A(R_i, R_j) = A(R_j, R_i)$. It also provides a relatively small θ_c away from the singular point so that the artifacts introduced to the nonsingular regions can be minimized.

IV. FREE ENERGY CALCULATION

We now derive formulas for calculating the free energy of the whole system. Elastic energy has already been calculated in the last section. We next evaluate the nonelastic parts of the free energy of the surface steps. We assume isotropic step energy and our calculations are based on steps along the (100) direction which is most convenient to analyze. The step formation energy per lattice site for the lattice model used in our KMC simulation is $\gamma_1/2 + \gamma_2$ from simple bond counting. Considering also the entropic contribution of kinks of arbitrary depth [34], the step free energy per unit length σ_1 for a 2D island is found to be

$$\sigma_1 = \frac{1}{a_s} \left\{ \frac{\gamma_1}{2} + \gamma_2 - kT \ln\left[1 + \frac{2e^{-(\gamma_1/2 + \gamma_2)/kT}}{1 - e^{-(\gamma_1/2 + \gamma_2)/kT}}\right] \right\}. \tag{12}$$

For a 3D stepped mound, mutual steric hindrance between adjacent steps leads to considerable effective step repulsion. Its strength is known to decay with the step separation ΔR as

ΔR^{-2} [35]. Noting also that the entropic term due the kinks should vanishes as ΔR approaches a_s, the free energy per unit length σ_n for steps in an n-layer island ($n \geq 2$) is instead approximated by

$$\sigma_n = \frac{1}{a_s} \left\{ \frac{\gamma_1}{2} + \gamma_2 - kT \left(1 - \frac{a_s^2}{\Delta R^2} \right) \right.$$
$$\left. \times \ln \left[1 + \frac{2e^{-(\gamma_1/2 + \gamma_2)/kT}}{1 - e^{-(\gamma_1/2 + \gamma_2)/kT}} \right] \right\}. \quad (13)$$

Summing up the elastic energy and the step energy, the total free energy of an n-layer island ($n \geq 1$) is

$$F_I(\{R_i\}) = 2\pi\sigma_n \sum_{i=1}^{n} R_i + E_s(\{R_i\}). \quad (14)$$

In particular for $n \geq 3$, we have assumed a truncated cone geometry with a uniform step spacing ΔR so that σ_n is constant for all layers, although both ΔR and σ_n still depend on the island height n. For 2D islands ($n = 1$), it reduces to the well known result [3]

$$F_I(R) = 2\pi R \left(\sigma_1 - \zeta \ln \frac{R}{a_r} \right). \quad (15)$$

Besides 2D or 3D islands, there are also adatoms on the substrate as well as on the islands. Their free energy contribution will now be studied. Dimers and other subcritical islands are few in number and are neglected. In our KMC simulation, elastic couplings of adatoms are neglected. The formation energy of an adatom is

$$E_{ad} = 2\gamma_1 + 2\gamma_2 - E_s^0, \quad (16)$$

where $E_s^0 = Y\varepsilon^2 a_s^3/(1-\nu)$ is the strain energy of a film atom in the homogeneously strained state. For an adatom density ρ, the entropy per site is $kT[\rho \ln \rho + (1-\rho)\ln(1-\rho)]$. At small ρ, the free-energy contribution of the adatoms is

$$F_{ad}(\rho) = L^2[\rho E_{ad} + (\rho \ln \rho - \rho)kT], \quad (17)$$

where L^2 is the number of lattice sites on the substrate.

The total free energy of the complete system with adatom density ρ and an island with n layers of radii $\{R_i\}$ is given by

$$F_S(\rho, \{R_i\}) = F_I(\{R_i\}) - kT \ln L^2 + F_{ad}(\rho), \quad (18)$$

where the term $kT \ln L^2$ accounts for the positional entropy of the island. Limiting to an n-layer island at a film material coverage θ, the free energy becomes

$$F_S(\theta, n) = \text{Min}\{F_S(\rho, \{R_i\})\}_{\rho, \{R_i\}}, \quad (19)$$

where Min denotes minimization w.r.t. ρ and $\{R_i\}$ under the constraint

$$\theta L^2 = \rho L^2 + N_I, \quad (20)$$

where $N_I = \pi \sum_{i=1}^{n} R_i^2/a_s^2$ is the number of atoms in the island. For simplicity, we only consider conelike or truncated conelike islands with a uniform step spacing ΔR so that the minimization is performed in general over the variables ρ, R_n, and ΔR.
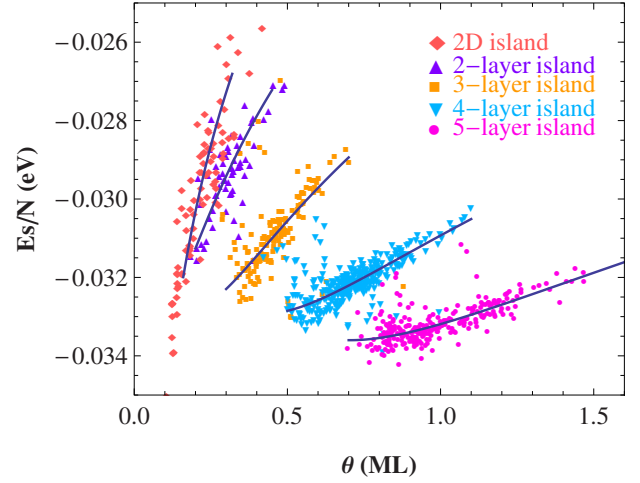

FIG. 2. (Color online) Plot of the strain energy per atom E_s/N against coverage θ from simulations (symbols) at deposition rates 1, 3, and 10 ML s^{-1}. The island height is inferred from the measured maximum surface height. The solid lines represent fitted curves using Eqs. (5) and (7).

Technically, the minimization in Eq. (19) is most conveniently carried out by adopting the chemical potential μ, rather than θ as an independent parameter. This is because thermodynamic theory implies $\rho \simeq e^{-(E_{ad}-\mu)/kT}$ and $\mu = dF_I(\{R_i\})/dN_I$ using which both θ and $F_S(\theta, n)$ are easily computable for any given μ using Eqs. (18)–(20).

V. APPLICATION TO KINETIC MONTE CARLO RESULTS

We have performed 6 independent runs for each of the deposition rates $R = 1$, 3 and 10 ML s^{-1}. We periodically calculate the strain relaxation energy E_s of the film-substrate system by comparing the total strain energy stored in all springs at mechanical equilibrium with that in the homogeneously strained state [21]. Figure 2 plots the strain energy per atom E_s/N against the film material coverage θ for all 18 runs, where $N = L^2\theta$ is the number of deposited atoms. Each data point results from averaging over 10 measurements of E_s in a given run taken during the deposition of about 0.02 MLs.

As observed in Fig. 2, E_s/N increases continuously upon deposition except at a few points where it drops abruptly. To understand this trend, we have simultaneously computed the number of layers n in the dominant island. Specifically, for each data point, we approximate $n+1$ by the maximum surface height during all the 30 associated measurements. Note that the offset one accounts for adatoms on the top layer which is not counted as a completed layer. The value n is indicated by the symbol representing the data point in Fig. 2. It is now clear that the abrupt drops in E_s/N coincide with the nucleation of new layers. Our data can then be interpreted as follow. The elastic energy of the system E_s is dominated by the largest island. During deposition, an island grows laterally and E_s/N increases toward zero gradually as the strain relaxation becomes increasingly inefficient. Periodically when the top layer becomes sufficiently spacious,

TABLE I. Effective elastic and geometrical parameters for n-layer islands from self-consistent strain energy fit and free-energy minimization.

Island height, n	ε (%)	$a_r(n)$	ΔR
1	11.6	$0.644a_s$	
2	12.3	$1.121a_s$	$1.706a_s$
3	11.0	$1.234a_s$	$1.383a_s$
4	10.3	$1.589a_s$	$1.233a_s$
5	9.59	$1.779a_s$	$1.131a_s$

upper-layer nucleation occurs. This enhances the effectiveness of the strain relaxation and induces and abrupt drop in E_s/N.

In Fig. 2, data from runs at rates 1, 3, and 10 ML s^{-1} basically coincide within statistical fluctuations and again indicates that growth proceeds close to the quasiequilibrium limit. More careful inspection reveals that E_s/N drops at slightly larger values of the coverage θ for some realizations reflecting the random nature of the upper-layer nucleation process. The spread is also more significant for the fastest 10 ML s^{-1} indicating that the slow deposition limit is only marginally valid at this deposition rate.

We next compare the strain energy E_s computed from our simulation with Eqs. (5) and (7) from continuum theory. From visual inspection of the morphological evolution like that in Fig. 1, there are typically 3 single-layer islands in the simulated system right before the 2D to 3D transition. Once a 3D island has developed, it dominates over the other islands which then vanish quickly. Therefore, we compare our strain energy data in the 2D case using Eq. (5) by considering 3 noninteracting islands of equal radius. In the 3D cases, we fit the data to Eq. (7) considering a single truncated cone. The results are shown as solid lines in Fig. 2 and the fitted parameters ε and $a_r(n)$ are listed in Table I. Note that we have adopted tunable effective values ε for the lattice misfit. The fitted values deviate slight from the nominal value 8% used in the simulations. We attribute the discrepancy to discretization effects caused by the sharp step edges surrounding each layer. Table I also lists values for the step separation ΔR. They are equilibrium values which minimizes the island free energy F_I defined in Eq. (14). Since the minimized value of ΔR depends on the fitted values of ε and $a_r(n)$ and vice versa, more precisely we have performed the strain energy fit and the island free-energy minimization self-consistently and the numerical procedure converges after several iterations.

From Table I, each of ε, $a_r(n)$, and ΔR depends on the island height n monotonically. These trends can be easily explained as follows. First, ΔR decreases with n meaning that taller islands have steeper sidewalls. This is because the larger strain energy associated with a tall island dominates over entropic repulsion described by the third term in Eq. (13). It can hence squeeze the steps more closely together. This is consistent with our simulation results as can be observed in Fig. 1. Experimentally, stepped mounds are also known to attain steeper inclinations gradually as growth proceeds [9,11]. Next, the effective misfit ε is considerably
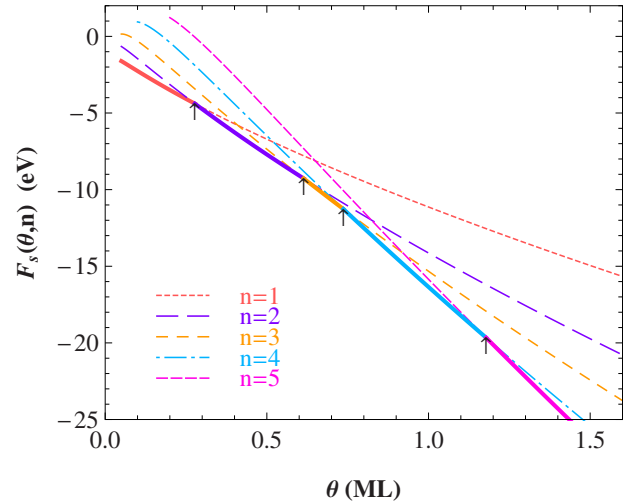

FIG. 3. (Color online) Plot of the total free energy $F_S(\theta, n)$ of a system with an n-layer island against coverage θ (dashed lines). The lowest values of F_S characterizing equilibrium states are indicated by thick solid lines.

larger than the nominal value of 8%. The discrepancy is due to the application of the continuum elasticity description to the discrete cubic lattice. It is particularly significant for thin islands as the misfit stress essentially acts very locally on the edge of each atomic layer of the islands. For taller islands, the discrepancy decreases as it crosses over to the continuum limit. We expect that the limited accuracy of the small slope approximation used in our theory also contribute partly to the decreases of ε with respect to n. In fact, the strain energy of an island with a high aspect ratio at large n are known to be overestimated in the small slope approximation [36]. Finally, the cutoff parameters $a_r(n)$ is expected to be a constant of the order a_s only for 2D islands or multilayered islands with large step separation ΔR so that the layers become noninteracting elastically. For the opposite case of a cylindrical island with $\Delta R=0$ so that $R_1=\cdots=R_n$, Eq. (7) reduces to $E_s[(R_i)]=-2\pi n^2 R_1\zeta \ln[R_1/a_r(n)]$. Alternatively, an n-layer cylindrical island is essentially similar to a 2D island and a proper rescaling of Eq. (5) gives $E_s[(R_i)]=-2\pi n^2 R_1\zeta \ln[R_1/na_r(1)]$. A comparison of the two expressions immediately gives $a_r(n)=na_r(1)$. For our simulation, ΔR is finite and hence $a_r(n)$ increases more moderately with n.

The free energy $F_S(\theta, n)$ of the system as a function of the coverage θ for various island height n then follows from Eq. (18) using parameters in Table I. Figure 3 shows the result which is in agreement with a schematic sketch motivated by experimental observations in Ref. [11]. For a given θ, the equilibrium island height n is identified easily as the one which minimizes the free energy $F_S(\theta, n)$ as indicated by the thick solid lines. We also observe that the equilibrium value of n increases sequentially from 1 onwards as θ increases. Therefore, for sufficiently slow deposition in the quasiequilibrium regime, islands form via a layer-by-layer nucleation mechanism in which a sequence of distinct upper-layer nucleation events occur one after another and each of them increases n by unity. Values of the critical coverage beyond which the corresponding upper-layer nucleation can occur

TABLE II. Properties of upper-layer nucleation on an n-layer island.

Island height, n	θ (ML)	R_n^*	R_{n+1}^*	E_b (eV)	τ (s)
2	0.614	$8.97a_s$	$2.53a_s$	0.521	0.00457
3	0.737	$7.41a_s$	$2.43a_s$	0.563	0.0141
4	1.18	$7.79a_s$	$2.62a_s$	0.689	0.147

are indicated by arrows in Fig. 3 and listed in Table II. The predicted critical coverages are in reasonable agreement with the positions of the abrupt drops in E_s/N in Fig. 2. This layer-by-layer nucleation mechanism is in agreement with experimental results on the evolution of stepped mounds at the initial stage of island formation [11,12].

We now study the dynamics of upper-layer nucleation. We first introduce a reaction parameter ϕ so that $\phi=0$ and 1 correspond respectively to the initial metastable n-layer island and the final $(n+1)$-layer island. Intermediate values of ϕ characterize transient island states. We assume for simplicity that all these islands have the same mass which is indeed a good approximation for $n \geq 2$ considered here. In the new top layer, the number of atoms is assumed to be linearly interpolated between the initial and the final values, so that the radius follows $R_{n+1}(\phi) = \sqrt{\phi} R_{n+1}^f$, where R_{n+1}^f denotes the final stable value. The remaining atoms belongs to the n lower layers which takes the geometry of a truncated cone. The step separation $\Delta R(\phi)$ for the n lower layers, the effective misfit $\epsilon(\phi)$, and the cutoff parameter $a_r(\phi)$ are all linearly interpolated between the initial and final equilibrium values from Table I. The island free energy $F_S(\phi)$ as a function of ϕ for each transition is then calculated. As an example, Fig. 4 plots $F_S(\phi)$ versus ϕ for $n=2$ corresponding to a two-layer to three-layer island transition. It shows the existence of an energy barrier [37]. The barrier height E_b and the associated layer radii R_n^* and R_{n+1}^* in the critical islands are calculated and listed in Table II. There are typically about

20 atoms in the 2D upper-layer nucleus, in contrast to only a few atoms often considered for other systems [38].

Using standard nucleation theory [39] the average upper-layer nucleation time τ can be estimated and we get

$$\tau = \frac{1}{zf^*c^*N_c}. \tag{21}$$

Here, $c^* \simeq e^{-E_b/kT}$ is the critical top-layer nucleus concentration and $N_c = \pi(R_n^{*2} - R_{n+1}^{*2})/a_s^2$ denotes the number of possible nucleation sites. Also, $f^* = \pi R_{n+1}^* a_s^{-3} D \rho$ is the adatom attachment rate where $D = D_0 e^{-E_a/kT}$ is the adatom diffusion coefficient with $E_a = 0.67$ eV and $D_0 = 3.83 \times 10^{13}$ A^2 s^{-1} for our KMC model. The Zeldovich factor z in Eq. (21) equals $z = \sqrt{-F''/2\pi kT}$ where we have defined $F'' = d^2 F(\phi)/ds^2$ evaluated at ϕ^* with $s = \pi R_{n+1}^2(\phi)/a_s^2$ denoting the number of atoms in the 2D embryo. Table II also lists the estimated nucleation time τ hence obtained. We note that τ is in general smaller than the total deposition time in our simulations and this justifies the quasiequilibrium nature of the island evolution in our simulations.

VI. DISCUSSIONS

KMC simulations in 3D with realistic elastic energies such as those performed here are computationally intensive and studies are limited to large misfits such as 8% associated with small island sizes [14,22]. Generic 3D nucleation associated with 3D critical embryo has not been observed. Nevertheless, direct experimental evidence on 3D nucleation for Ge films with 4% misfit is also lacking, although this can be due to experimental challenges associated with the short nucleation time, the small embryo size or simply the intrinsic instability of the intermediate states. The layer-by-layer nucleation pathway observed in KMC can be another possible description for the initial evolution of islands before faceting at high misfit and low temperature. Nevertheless, the theoretical framework proposed here is more general and can be applied to lower misfit regimes. At 1% misfit, atomic resolution images have clearly revealed emerging islands in the form of stepped mounds with facetted terraces [12]. Our theory can be a candidate for the description of their evolution. We also hope that this work can motivate further quantitative comparison between theory and experiments. For example, it will be interesting to extend experiments in Ref. [12] and measure the size distribution of the top 2D island as a function of the height of the stepped mound. This distribution provides important information about the top layer stability and also the growth dynamics. It is also readily predictable using our theory for a direct comparison.
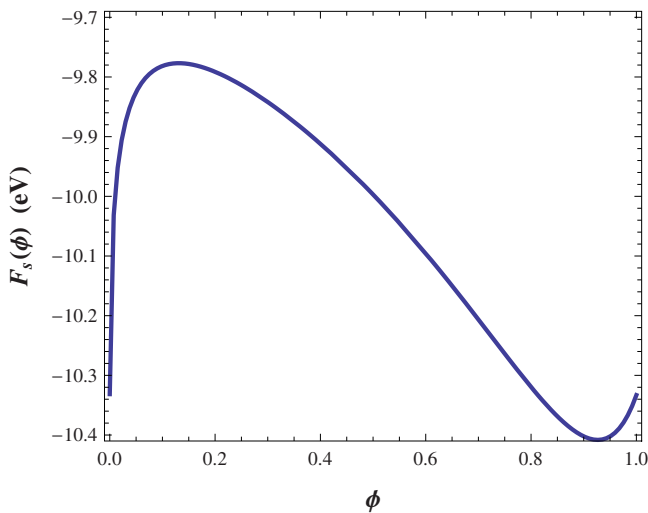

FIG. 4. (Color online) Plot of system free energy $F_S(\phi)$ against reaction parameter ϕ for upper-layer nucleation on a two-layer island at coverage $\theta=0.614$.

The layer-by-layer growth mode involves energetics driven island lateral expansion stages interrupted by upper-layer nucleations. After adding each layer, the island is stable until growing beyond a certain size and become metastable again. This is because our free energy calculation has shown that all n-layer islands studied are energetically stable at some coverage θ. Another possibility is that once a 2D island grows beyond a critical size, there is a kinetic limited cascade of upper-layer nucleation events at practically constant island size until the island becomes stable again [40]. The island development process is then limited essentially by a single 2D to 3D energy barrier. This picture does not describe our KMC simulations. However, we did arrive theoretically at such a result when neglecting the entropic step repulsion term in Eq. (13) so that islands of thickness 2 and 3 MLs are metastable for all island sizes. Entropic step repulsion hence is also a relevant factor in selecting the true growth mechanism.

3D KMC simulations have demonstrated island formation via either surface instability at 1000 K [14] or the layer-by-layer nucleation mechanism at 600 K as studied in detail here. At intermediate temperatures, visual inspection of the morphological evolution indicates rather smooth crossovers between the two set of features. From a theoretical point of view, at 600 K the upper-layer nucleation energy barrier is significantly larger than kT. Upper-layer nucleation hence introduces noticeable ensemble randomness to the island evolution as observed here and on pit formation in Ref. [14]. For higher temperatures, it is easy to deduce from our theory that the upper-layer nucleation barrier decreases due to the lower free energy of the surface steps. Upper-layer nucleation can therefore become a fast process compared with the lateral expansion of the islands. Island will then grow at more steady rates with suppressed ensemble fluctuations. Island formation thus lacks not only 3D barrier but practically also any significant 2D barrier and becomes essentially nucleationless as proposed in Ref. [11]. At still higher tempera-ture, the evolution should further converges to standard surface instability induced growth as surface step free energy further decreases and approaches zero. It will be interesting to apply our theory to describe these temperature induced crossovers between roughening modes quantitatively.

In summary, we have demonstrated both computationally and analytically a layer-by-layer nucleation mechanism for the self-assembly of 3D islands in strained heteroepitaxy at temperature below the surface roughening transition. KMC simulations at 600 K under slow deposition conditions show that the island morphologies depend mainly on the island size and is very much independent of the deposition rates. The results imply a quasiequilibrium layer-by-layer growth mode with independent and distinct upper-layer nucleation events and this simplifies analytically description. In our theory, islands are treated as axisymmetric stepped mounds. The elastic strain energy is calculated under the small-slope approximation. We have also considered step meandering entropy due to step kinks as well as step-step repulsion of entropic origin. Effective values of the lattice misfit and lattice cutoff parameter are extracted by fitting to KMC simulation results. Using these values, our theory explains a layer-by-layer nucleation mechanism for the development of 3D islands for slow deposition in the quasiequilibrium regime. Islands can be approximated by their equilibrium geometries as dictated by the material coverage. As deposition proceeds, a sequence of independent 2D upper-layer nucleation occurs while the layers expand laterally in between these events. The associated nucleation barriers, average nucleation times, critical upper-layer 2D island sizes, and transition material coverage are estimated. Our theory provides a satisfactory quantitative description of the island formation process in the KMC simulation.

[1] P. Politi, G. Grenet, A. Marty, A. Ponchet, and J. Villain, Phys. Rep. **324**, 271 (2000).

[2] A. Pimpinelli and J. Villain, *Physics of Crystal Growth* (Cambridge University Press, Cambridge, New York, 1998).

[3] V. A. Shchukin, N. N. Ledentsov, and D. Bimberg, *Epitaxy of Nanostructures* (Springer, New York, 2003).

[4] L. B. Freund and S. Suresh, *Thin Film Materials, Stress, Defect Formation and Surface Evolution* (Cambridge, Cambridge, England, 2003).

[5] Y.-W. Mo, D. E. Savage, B. S. Swartzentruber, and M. G. Lagally, Phys. Rev. Lett. **65**, 1020 (1990).

[6] J. Stangl, V. Holý, and G. Bauer, Rev. Mod. Phys. **76**, 725 (2004).

[7] J. Tersoff and F. K. LeGoues, Phys. Rev. Lett. **72**, 3570 (1994).

[8] A. Vailionis, B. Cho, G. Glass, P. Desjardins, D. G. Cahill, and J. E. Greene, Phys. Rev. Lett. **85**, 3672 (2000).

[9] J. A. Floro, E. Chason, L. B. Freund, R. D. Twesten, R. Q. Hwang, and G. A. Lucadamo, Phys. Rev. B **59**, 1990 (1999).

[10] J. Tersoff, B. J. Spencer, A. Rastelli, and H. von Känel, Phys. Rev. Lett. **89**, 196104 (2002).

[11] P. Sutter and M. G. Lagally, Phys. Rev. Lett. **84**, 4637 (2000).

[12] P. Sutter, P. Zahl, and E. Sutter, Appl. Phys. Lett. **82**, 3454 (2003).

[13] R. M. Tromp, F. M. Ross, and M. C. Reuter, Phys. Rev. Lett. **84**, 4641 (2000).

[14] M. T. Lung, C.-H. Lam, and L. M. Sander, Phys. Rev. Lett. **95**, 086102 (2005).

[15] B. G. Orr, D. Kessler, C. W. Snyder, and L. Sander, EPL **19**, 33 (1992).

[16] C.-H. Lam, C.-K. Lee, and L. M. Sander, Phys. Rev. Lett. **89**, 216102 (2002).

[17] J. L. Gray, R. Hull, C.-H. Lam, P. Sutter, J. Means, and J. A. Floro, Phys. Rev. B **72**, 155323 (2005).

[18] T. P. Schulze and P. Smereka, J. Mech. Phys. Solids **57**, 521 (2009).

[19] A. Baskaran, J. Devita, and P. Smereka, Continuum Mech. Thermodyn. **22**, 1 (2010).

[20] C.-H. Lam and M. T. Lung, Int. J. Mod. Phys. B **21**, 4219 (2007).

[21] C.-H. Lam, M. T. Lung, and L. M. Sander, J. Sci. Comput. **37**, 73 (2008).

[22] G. Russo and P. Smereka, J. Comput. Phys. **214**, 809 (2006).

[23] Y. Tu and J. Tersoff, Phys. Rev. Lett. **93**, 216101 (2004).

[24] Z. Huang, T. Zhou, and C.-h. Chiu, Phys. Rev. Lett. **98**, 196102 (2007).

[25] Y. Fujikawa, K. Akiyama, T. Nagao, T. Sakurai, M. G. Lagally, T. Hashimoto, Y. Morikawa, and K. Terakura, Phys. Rev. Lett. **88**, 176101 (2002).

[26] G.-H. Lu, M. Cuma, and F. Liu, Phys. Rev. B **72**, 125415 (2005).

[27] S. Cereda and F. Montalenti, Phys. Rev. B **75**, 195321 (2007).

[28] M. Biehl, F. Much, and C. Vey, Int. Numer. Math. **149**, 41 (2005).

[29] C. M. Retford, M. Asta, M. J. Miksis, P. W. Voorhees, and E. B. Webb III, Phys. Rev. B **75**, 075311 (2007).

[30] J. A. Floro, M. B. Sinclair, E. Chason, L. B. Freund, R. D. Twesten, R. Q. Hwang, and G. A. Lucadamo, Phys. Rev. Lett.

[31] J. Tersoff and R. M. Tromp, Phys. Rev. Lett. **70**, 2782 (1993).

[32] A. I. Lurie, *Theory of Elasticity* (Springer, Berlin, 2005).

[33] R. Xiang, Master's thesis, The Hong Kong Polytechnic University, 2008.

[34] H. J. W. Zandvliet, F. R. van Dijk, and B. Poelsema, Phys. Rev. B **72**, 113412 (2005).

[35] H. C. Jeong and E. D. Williams, Surf. Sci. Rep. **34**, 171 (1999).

[36] D. Vanderbilt and L. K. Wickham, in *Evolution of Thin-Film and Surface Microstructure*, MRS Symposia Proceedings No. 202, edited by C. V. Thompson *et al.* (Materials Research Society, Pittsburgh, 1991), pp. 555–560.

[37] We note that the minimum of $F_S(\phi)$ indeed occurs at ϕ slightly smaller than 1. This simply indicates that the final equilibrium island deviates slightly from the truncated conical geometry, but for simplicity such deviation is neglected in our main calculations.

[38] J. G. Amar and F. Family, Phys. Rev. Lett. **74**, 2066 (1995).

[39] D. Kashchiev, *Nucleation: Basic Theory with Applications* (Oxford, New York, 2000).

[40] K. E. Khor and S. Das Sarma, Phys. Rev. B **62**, 16657 (2000).

[84], 701 (2000).